Role of hydrogen loading and glass composition on the defects generated by the femtosecond laser writing process of fiber Bragg gratings

Neil Troy,[1,*] Christopher W. Smelser,[2] and Denise M. Krol[1]

[1]*Department of Applied Science, University of California Davis, Davis, California 95616, USA*
[2]*Communications Research Centre Canada, 3701 Carling Ave., P.O. Box 11490, Station H, Ottawa, Ontario K2H 8S2, Canada*
ntroy@ucdavis.edu

Abstract: The creation of fiber Bragg gratings (FBGs) in optical fibers by laser irradiation causes the formation of defects in the modified glass. We have used confocal fluorescence spectroscopy to identify the location and types of defects formed after writing FBGs with the femtosecond laser phase mask technique. Our results show that non-bridging oxygen hole centers (NBOHCs) and self-trapped excitons (E_δ') are formed throughout all-silica core Sumitomo Z-fiber. Similar defects are observed for Ge-doped silica fiber, Corning SMF-28, but in this case the relative concentrations of NBOHC and E_δ' vary from the core to the cladding. In both fibers, hydrogen loading prior to irradiation appears to passivate the defects except in the Ge-doped core where the NBOHC defects persist.

OCIS codes: (230.1480) Bragg reflectors; (050.0050) Diffraction and gratings; (320.7140) Ultrafast processes in fibers; (350.3390) Laser materials processing; (160.2750) Glass and other amorphous materials; (320.2250) Femtosecond phenomena.

References and links

1. K. Miura, J. Qiu, H. Inouye, T. Mitsuyu, and K. Hirao, "Photowritten optical waveguides in various glasses with ultrashort pulse laser," Appl. Phys. Lett. **71**(23), 3329–3331 (1997).
2. S. Nolte, M. Will, J. Burghoff, and A. Tuennermann, "Femtosecond waveguide writing: a new avenue to three-dimensional integrated optics," Appl. Phys., A Mater. Sci. Process. **77**(1), 109–111 (2003).
3. T. Sikorski, A. A. Said, P. Bado, R. Maynard, C. Florea, and K. A. Winick, "Optical waveguide amplifier in Nd-doped glass written with near-IR femtosecond laser pulses," Electron. Lett. **36**(3), 226–227 (2000).
4. S. Taccheo, G. Della Valle, R. Osellame, G. Cerullo, N. Chiodo, P. Laporta, O. Svelto, A. Killi, U. Morgner, M. Lederer, and D. Kopf, "Er:Yb-doped waveguide laser fabricated by femtosecond laser pulses," Opt. Lett. **29**(22), 2626–2628 (2004).
5. S. J. Mihailov, D. Grobnic, C. W. Smelser, P. Lu, R. B. Walker, and H. Ding, "Bragg grating inscription in various optical fibers with femtosecond infrared lasers and a phase mask," Opt. Mater. Express **1**(4), 754–765 (2011).
6. D. Grobnic, C. W. Smelser, S. J. Mihailov, R. B. Walker, and P. Lu, "Fiber Bragg gratings with suppressed cladding modes made in SMF-28 with a femtosecond IR laser and a phase mask," IEEE Photon. Technol. Lett. **16**(8), 1864–1866 (2004).
7. C. W. Smelser, S. J. Mihailov, and D. Grobnic, "Hydrogen loading for fiber grating writing with a femtosecond laser and a phase mask," Opt. Lett. **29**(18), 2127–2129 (2004).
8. B. L. Zhang and K. Raghavachari, "Microscopic reaction mechanisms in hydrogen-loaded germanosilicate fibers: formation of divalent Ge defects," Phys. Rev. B Condens. Matter **51**(12), 7946–7949 (1995).
9. B. I. Greene, D. M. Krol, S. G. Kosinski, P. J. Lemaire, and P. N. Saeta, "Thermal and photo-initiated reactions of H_2 with germanosilicate optical fibers," J. Non-Cryst. Solids **168**(1-2), 195–199 (1994).
10. M. Fujimaki, T. Kasahara, S. Shimoto, N. Miyazaki, S. Tokuhiro, K. Soo Seol, and Y. Ohki, "Structural changes induced by KrF excimer laser photons in H_2-loaded Ge-doped SiO_2 glass," Phys. Rev. B **60**(7), 4682–4687 (1999).
11. W. J. Reichman, J. W. Chan, C. W. Smelser, S. J. Mihailov, and D. M. Krol, "Spectroscopic characterization of different femtosecond laser modification regimes in fused silica," J. Opt. Soc. Am. B **24**(7), 1627–1632 (2007).
12. C. W. Smelser, S. J. Mihailov, and D. Grobnic, "Formation of Type I-IR and Type II-IR gratings with an ultrafast IR laser and a phase mask," Opt. Express **13**(14), 5377–5386 (2005).
13. J. Albert, M. Fokine, and W. Margulis, "Grating formation in pure silica-core fibers," Opt. Lett. **27**(10), 809–811 (2002).

#173851 - $15.00 USD Received 7 Aug 2012; revised 16 Oct 2012; accepted 17 Oct 2012; published 25 Oct 2012

14. K. Kajihara, L. Skuja, M. Hirano, and H. Hosono, "Formation and decay of nonbridging oxygen hole centers in SiO_2 glasses induced by F_2 laser irradiation: *in situ* observation using a pump and probe technique," Appl. Phys. Lett. **79**(12), 1757–1759 (2001).
15. L. Skuja, H. Hosono, M. Mizuguchi, D. Guttler, and A. Silin, "Site-selective study of the 1.8 eV luminescence band in glassy GeO_2," J. Lumin. **87–89**, 699–701 (2000).
16. S. Girard, J.-P. Meunier, Y. Ouerdane, A. Boukenter, B. Vincent, and A. Boudrioua, "Spatial distribution of the red luminescence in pristine, γ rays and ultraviolet-irradiated multimode optical fibers," Appl. Phys. Lett. **84**(21), 4215–4217 (2004).
17. Y. Ikuta, K. Kajihara, M. Hirano, S. Kikugawa, and H. Hosono, "Effects of H_2 impregnation on excimer-laser-induced oxygen-deficient center formation in synthetic SiO_2 glass," Appl. Phys. Lett. **80**(21), 3916–3918 (2002).
18. M. Mizuguchi, L. Skuja, H. Hosono, and T. Ogawa, "Photochemical processes induced by 157-nm light in H_2-impregnated glassy SiO_2:OH," Opt. Lett. **24**(13), 863–865 (1999).
19. K. P. Chen, P. R. Herman, R. Tam, and J. Zhang, "Rapid long-period grating formation in hydrogen-loaded fibre with 157 nm F_2-laser radiation," Electron. Lett. **36**(24), 2000–2001 (2000).
20. M. Essid, J. L. Brebner, J. Albert, and K. Awazu, "Difference in the behavior of oxygen deficient defects in Ge-doped silica optical fiber preforms under ArF and KrF excimer laser irradiation," J. Appl. Phys. **84**(8), 4193–4197 (1998).
21. D. P. Poulios, J. P. Spoonhower, and N. P. Bigelow, "Influence of oxygen deficiencies and hydrogen-loading on defect luminescence in irradiated Ge-doped silica glasses," J. Lumin. **101**(1-2), 23–33 (2003).
22. K. Awazu, K. Muta, and H. Kawazoe, "Formation mechanism of hydrogen-associated defect with an 11.9 mT doublet in electron spin resonance and red luminescence in $9SiO_2$:GeO_2 fibers," J. Appl. Phys. **74**(4), 2237–2240 (1993).

1. Introduction

By focusing intense femtosecond laser pulses into glasses, one can cause a permanent modification in the index of refraction to take place in the focal volume of the laser pulse [1]. This technique has been used to create passive optical devices like waveguides and splitters as well as active devices like amplifiers and lasers all of which are completely embedded in a piece of glass [1–4]. The femtosecond writing process has also been applied to the production of fiber Bragg gratings (FBGs) with much success. In many cases femtosecond laser-written FBGs, hereafter referred to as fs-FBGs, perform better and can be written in more materials than the standard ultraviolet (UV) written ones [5].

Fundamentally, femtosecond lasers as a writing source for FBGs offer some advantages over UV inscription. The UV writing process is based upon a one-photon absorption process across the bandgap of the glass, typically E_g ~4-5 eV for oxide glasses. This absorption process can lead to a change in the refractive index of the irradiated material. A common strategy is to use photosensitizing agents, such as germanium in the core of the optical fiber, to create absorption bands for the UV light source. This also limits the induced refractive index changes to the core of the optical fiber. Femtosecond laser material modification is fundamentally different from UV modification as it is initiated through a highly nonlinear multi-photon interaction. The photon energy of the light, E_p~1.5 eV for a typical Ti:sapphire (Ti:S) laser, is far below the bandgap of a typical oxide glass and, thus, one-photon absorption does not take place. Energy from the laser pulse can only be deposited into the material through the simultaneous absorption of n photons, such that $nE_p > E_g$. Due to this highly nonlinear modification scheme, femtosecond FBG writing is confined to the small focal volume of the laser and requires no special doping of the fiber. This not only allows grating inscription in various oxide based glasses but also allows for the suppression of cladding modes, as the modification is no longer limited to the core of the fiber [6]. It has also been shown that, similar to what is observed for UV writing, preloading the fibers with molecular hydrogen before irradiation reduces the modification threshold and produces gratings that are both stronger and more temperature resistant [7].

Unfortunately, the process of creating FBGs in fibers with UV and femtosecond lasers is still not completely understood. It is clear that in both FBG writing processes the writing laser creates defects in the glass network. In the case of the UV modification of silica-based glass fibers, much work has been done on identifying the kinds of defects generated [8–10].

#173851 - $15.00 USD Received 7 Aug 2012; revised 16 Oct 2012; accepted 17 Oct 2012; published 25 Oct 2012

However, few studies exist for fs-FBGs. For all-silica core fibers we have shown distinct differences in the fluorescence (FL) signature for type-I and type-II gratings [11]. Type-I gratings, which have low thermal stability, were dominated by a fluorescence signal peaked at 530 nm; type-II gratings, which are stable up to 1000°C, show strong FL peaked at 650 nm from non-bridging oxygen hole centers (NBOHCs).

In the present study, we have extended our earlier work to include the effect of hydrogen loading on fs-FBGs in all-silica core fibers. In addition, we have investigated the defects associated with fs-FBGs in Ge-doped silica fibers (Corning SMF-28) both with and without hydrogen loading, since this is a more common type of fiber used for UV gratings. In particular, we are interested in comparing the types of defects generated with both grating inscription techniques. By using the high spatial resolution provided by confocal FL microscopy, we can identify the species of defects in the FBGs as well as their location within the fiber. We use these defect FL signatures to better understand the modification process but also to try to determine the roles of hydrogen loading and Ge in the creation of FBGs with a femtosecond laser source.

2. Experimental procedure

Fs-FBGs were formed in both Corning SMF-28 and Sumitomo Z-fiber by focusing the pulsed output of an amplified ultrafast laser (Spectra-Physics Spitfire) through a 3.14 μm pitch phase mask onto the target fiber to create third-order Bragg gratings for 1550 nm light. A 30 mm focal length cylindrical lens was positioned such that the line focus was parallel to and at the fiber's core. The various phase mask modes produce an interference pattern that is then imprinted within the fiber as seen in Fig. 1. The target fiber was placed ~3 mm behind the phase mask and the beam was scanned vertically ± 10 μm to allow for maximal coverage of the core region of the fiber. The temporal pulse width of the laser was ~125 fs. The repetition rate of the laser was set at 100 Hz and the pulse energy was 900 μJ. With these parameters the intensity of the laser at the fiber core was ~$2x10^{13}$ W/cm^2, below that required for type-II damage grating formation [12]. The transmission loss at the Bragg wavelength of the grating was continuously monitored with a spectrum analyzer. The FBG writing process was stopped when the grating strength was measured at ~20 dB for 1550 nm light, see Table 1. This generally resulted in grating structures ~5 mm in length with a modulation in refractive index of ~1 x 10^{-4}. For hydrogen loading, the fibers were placed in a high-pressure hydrogen chamber at 2500 psi for 2 weeks at room temperature. After grating inscription the fiber was left at room temperature and pressure for 2 weeks to allow the hydrogen to outgas.

Table 1. Number of fs-Pulses Required for Bragg Grating Strength in Various Fibers

	SMF-28		Z-fiber	
	w/o H_2	w/ H_2	w/o H_2	w/ H_2
Grating strength	20 dB	18 dB	20 dB	22 dB
Approx. number of fs-pulses	16,000	16,000	7,000	4,000

After FBGs were written, they were investigated for defect FL using a scanning confocal spectrometer. The excitation source was a CW 473 nm diode pumped solid-state laser (DHL-B150N). The fibers were investigated primarily from the side (same direction as the femtosecond irradiation). To further determine the spatial location of the defects some of the fibers were cleaved at the FBG and investigated for defect FL. To ensure tight focusing conditions for the side acquisitions, the excitation laser was focused with a Mitutoyo Plan Apochromatic 50x/0.55 objective through a cover slip and non-fluorescing immersion oil (Cargille FF) into the fiber. Cleaved fibers were investigated using the same microscope objective but without the immersion oil or cover slip. FL signals were then analyzed with an Oriel MS257 spectrometer equipped with a 300 lines/mm grating and a thermo-electrically

#173851 - $15.00 USD Received 7 Aug 2012; revised 16 Oct 2012; accepted 17 Oct 2012; published 25 Oct 2012

cooled CCD camera (Princeton Instruments, SPEC-10). All spectra presented were acquired with an identical excitation power of 5 mW, focusing conditions (objective listed above), and acquisition times of 1 second per spectrum.

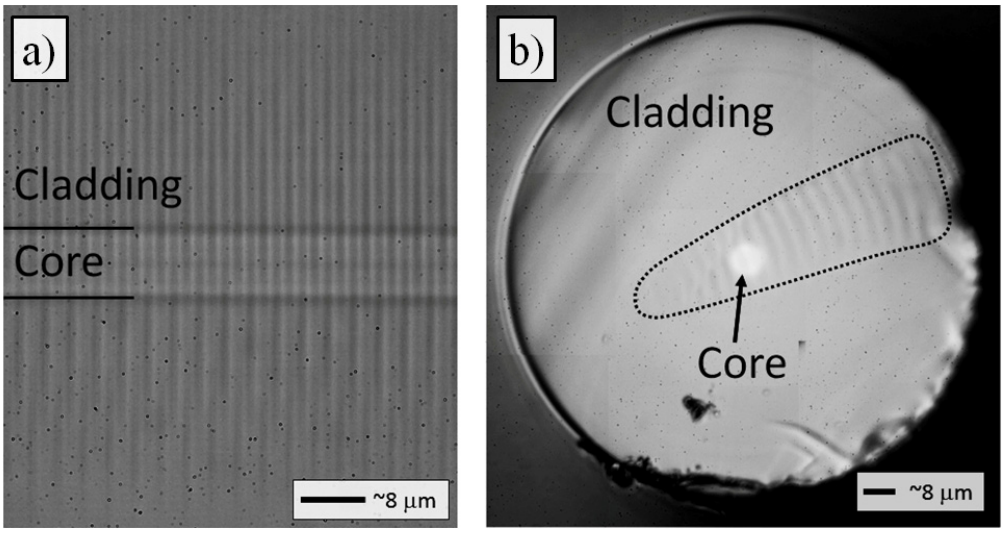

Fig. 1. White light transmission images of fs-FBG written in non-hydrogen loaded SMF-28 fiber viewed from the side through immersion oil (a) and viewed through a cleaved end (b). The dotted line in 1b highlights the modified region of the fiber. The core diameter is ~8.2 um in both images.

3. Results

Sumitomo Z-Fiber (all-silica core, F-doped cladding)

Figure 2(a) depicts the FL spectra from a fs-FBG modified core and cladding in an all-silica fiber without hydrogen loading. The strong feature centered at 530 nm and the weak but broad signal around 600-700 nm are very similar to our earlier results on type-I gratings in this fiber [11]. The 530 nm FL peak is due to self-trapped excitons (E_{δ}') in small Si-clusters and the broad peak centered at ~650 nm is due to non-bridging oxygen hole center (NBOHC) defects. Of note is that in this fiber we were not able to detect any difference in the FL signature whether it was from the modified core or the modified cladding even though the cladding is doped with fluorine.

The hydrogen-loaded all-silica fs-FBG was created with a noticeable reduction in femtosecond laser pulses, see Table 1. This result concurs with the work of Albert et. al., which showed that the loading of fibers with molecular hydrogen prior to irradiation with a UV laser at 193 nm allowed for a faster and stronger grating inscription process [13]. The lack of FL features, shown in Fig. 2(b), would indicate that the two defects previously identified are not present in this case. The effect of hydrogen loading on all-silica fibers and the lack of defect generation agrees well with the work done with UV inscribed modifications where the presence of hydrogen provides a passivation pathway for the defects that were created during the writing process [14].

#173851 - $15.00 USD Received 7 Aug 2012; revised 16 Oct 2012; accepted 17 Oct 2012; published 25 Oct 2012

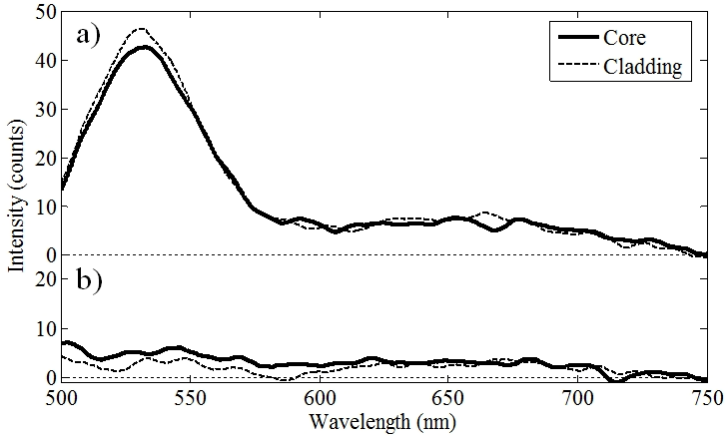

Fig. 2. Fluorescence spectra from Sumitomo Z-Fiber (all-silica-core) without (a) and with (b) hydrogen loading. The solid curve in each set represents the fluorescence from the core, while the dashed curve is the signal from the cladding.

Corning SMF-28 (Ge-doped core, all-silica cladding)

FL spectra were also gathered from a fs-FBG in SMF-28 fiber and are shown in Fig. 3. In this FBG we again note two distinct FL peaks, one centered at ~530 nm and one centered near 650-660 nm. There is a stark contrast in the FL intensities depending on the location within the fiber. The relative enhancement of the 650 nm and weakening of the 530 nm signal in the core is best seen in the FL maps of Fig. 4. These maps were created by fitting the FL data with two Gaussian peaks, one near 530 nm and one near 650 nm and mapping their normalized intensities. By comparing these FL maps with the white light image in Fig. 1(b) we see 530 nm FL throughout the modified regions, be it core or cladding, but a significant localization of the 650 nm FL to the core of the fiber.

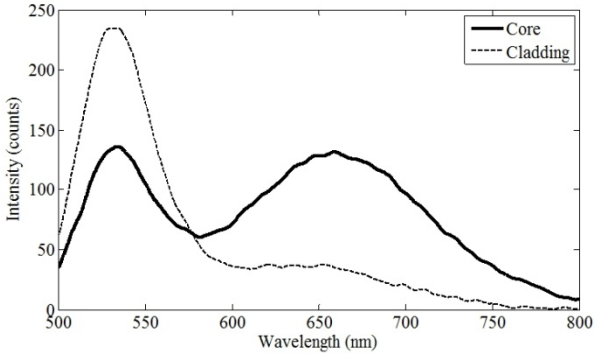

Fig. 3. Defect fluorescence from modified material in the core (solid curve) and cladding (dashed curve) of a non-hydrogen loaded SMF-28 fs-FBG. The relative intensity of the 530 nm and 650 nm fluorescence is dependent on the location within the fiber itself.

Concerning the cladding FL, Figs. 3 and 4 indicate a strong 530 nm peak and a weak 650 nm peak. In contrast to the Z-fiber that uses an all-silica-core and fluorine doping in the cladding, SMF-28 fibers have a Ge-doped core and all-silica-cladding. This means that the composition of the cladding of the SMF-28 fiber is similar to that of the Z-fiber's core. Based upon our prior interpretation, we again assign the strong 530 nm FL and weaker 650 nm FL to E_δ' defects and NBOHC defects, respectively. We suspect that the significant increase in FL intensity of the SMF-28 cladding compared to the Z-fiber core is likely due to the increased number of

#173851 - $15.00 USD Received 7 Aug 2012; revised 16 Oct 2012; accepted 17 Oct 2012; published 25 Oct 2012

femtosecond pulses used to modify the glass and a resulting increase in the number of defects present, as indicated in Table 1.

A complication arises in assigning defects in the core region due to the presence of germanium. Ge and Si form similar tetrahedral structures in the glass network and can form similar defects. The 530 nm FL is likely due to the E_δ' as these are related to silicon nanoclusters and we see no evidence in the literature of an equivalent Ge based defect FL in this range.

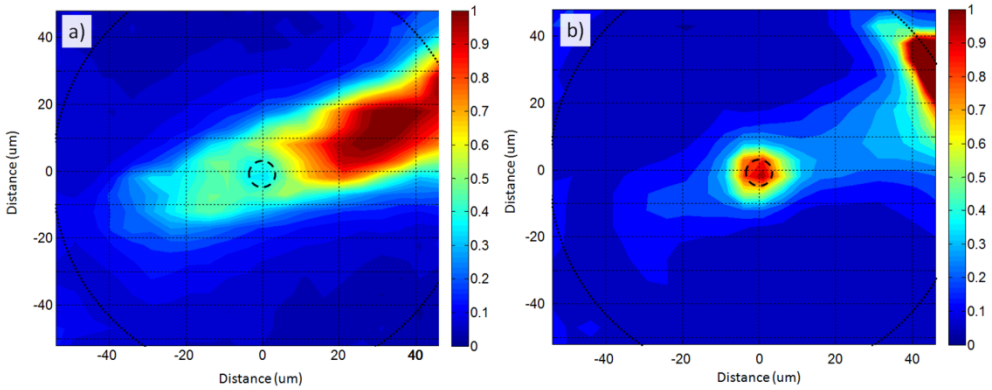

Fig. 4. Normalized maps of the fluorescence intensity from the 530 nm (a) and 650-660 nm (b) peaks in SMF-28 fiber without hydrogen loading. The small dashed circle represents the core (~8.2 um diameter) and the large dotted circle represents the edge of the cladding (125 um diameter).

The highly localized nature of the 650-660 nm peaks emitted from the core leads us to believe that Ge is playing a large role in defect generation in this region. In particular, it has been shown that NBOHC FL due to Si sites and Ge sites are very similar but their peak wavelengths are distinctly different at 645 nm (1.92 eV) and 667 nm (1.86 eV), respectively [15]. However, due to the contamination of the FL signal from the E_δ' defect we are not able to say definitively that the defects from the core are due to one or the other. In the case of UV irradiation of similar composition fibers it was shown that there is a high localization of photoluminescent defects in the core and that they are due to a mixture of Ge- and Si- NBOHC defects [16]. We would surmise that the signal we do detect is likely a mixture of the two different NBOHC defects as is the case for UV irradiation.

A similar fs-FBG was also created in a hydrogen-loaded SMF-28 fiber; the acquired FL spectra can be seen in Fig. 5. First, concerning the modified cladding there is no observable defect FL, as indicated by the flat dashed curve in Fig. 5. This corroborates well with the results of the hydrogen loaded Z-fiber since they are both all-silica and so the previous assertion that hydrogen allows for a passivation of these defects also applies to the SMF-28 cladding.

Looking at the core of the hydrogen-loaded SMF-28 fiber we note a large FL peak located at ~660 nm (solid curve in Fig. 5). Since there is no contamination from E_δ' defects we can accurately determine that this peak is centered at 660 nm. Since 660 nm is not the peak position for either of the two NBOHC species we can confidently say that this peak is due to the two overlapping signals of Si- and Ge-based NBOHC defects.

#173851 - $15.00 USD Received 7 Aug 2012; revised 16 Oct 2012; accepted 17 Oct 2012; published 25 Oct 2012

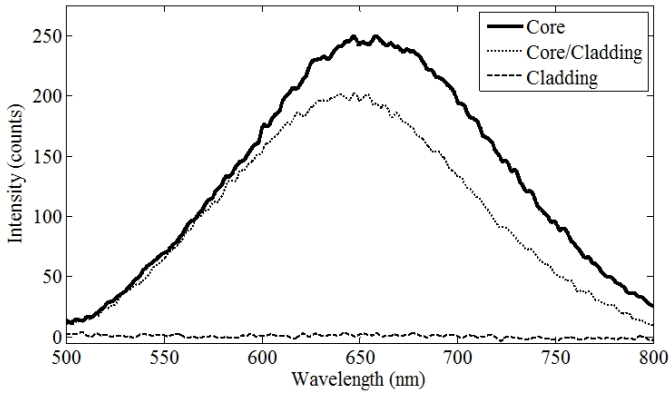

Fig. 5. Defect fluorescence from modified material in the core (solid curve), core/cladding interface (dotted curve), and modified cladding (dashed curve) in a hydrogen loaded SMF-28 fiber.

We observe a blue shift of the NBOHC FL near the core/cladding interface (dotted curve in Fig. 5). As previously stated, this FL is likely due to the two different species of NBOHC sites and a blue shift would indicate that more of the sites are related to Si-based NBOHC defects due to their shorter-wavelength emission at 645 nm. We note that, in contrast to what happens in the cladding as well as throughout the all-silica fiber, the NBOHC defects in the SMF-28 fiber core are not being passivated by hydrogen. Apparently the presence of Ge counteracts the passivation mechanism.

Table 2. The Defect FL Found in the Core and Cladding in Each Fiber with and without Hydrogen Loading*

	SMF-28		Z-fiber	
	w/o H_2	w/ H_2	w/o H_2	w/ H_2
Core defect FL (counts)	E_δ' (110) NBOHC (140)	NBOHC (270)	E_δ' (40) NBOHC (10)	None Detected
Cladding defect FL (counts)	E_δ' (240) NBOHC (40)	None Detected	E_δ' (40) NBOHC (10)	None Detected

*The values in parentheses represent the heights of the calculated Gaussian function used to fit the spectral data.

We have also compared the intensity of all of our results (cf. Table 2). Of interest is the increase of the number of NBOHC defects in the hydrogen-loaded SMF-28 fiber compared to an SMF-28 fiber without hydrogen treatment. Our results show an increase in red FL in hydrogen loaded Ge-doped silica fibers. This may be correlated with the fact that hydrogen loading of SMF-28 fibers reduces the modification threshold [7]. As can be seen from Table 1 both SMF-28 fibers investigated in this study have been irradiated identically. If the modification threshold is lower for the hydrogen-loaded fiber, we may consider this fiber to have experienced more of an effect from the laser compared to the non-hydrogen loaded fiber. This would likely lead to more defects being generated.

Finally, we discuss how defect formation with fs lasers compares with what has been observed with UV lasers. UV-written Bragg gratings are typically fabricated in Ge-doped fiber. In the case of all-silica fiber, gratings can be produced with ArF radiation at 193 nm [13] rather than with 248 nm KrF laser light typically used for Ge-doped fibers. Defect formation after exposure to 193 nm, or even shorter wavelength 157 nm light from a F_2 laser, has been studied primarily in bulk silica glasses, both with and without hydrogen loading [14,17,18]. The results are very similar to what we observe in our studies, i.e. the formation of NBOHC defects, which are observed for samples without H_2, is largely suppressed in samples that are hydrogen loaded. It is not surprising that these two different irradiation conditions yield the same defects, because in both cases a band-to-band transition is induced. In the case of UV light this occurs through a

#173851 - $15.00 USD Received 7 Aug 2012; revised 16 Oct 2012; accepted 17 Oct 2012; published 25 Oct 2012

one-photon process, as opposed to a multi-photon process in the case of fs-laser irradiation. For the Ge-doped SMF-28 fiber the UV results are less clear-cut. This is partly due to the fact that defect formation depends on the irradiation wavelength [19,20]. However, a FL band at 650 nm due to the formation of NBOHC defects has been established for a wide range of irradiation conditions [16]. As far as the effects of hydrogen loading are concerned, the increase in the red FL band that we observe here has also been reported for x-ray irradiation of hydrogen-loaded germanosilicate glasses and gamma ray irradiation of hydrogen-loaded Ge-doped fibers [21,22].

4. Summary

Femtosecond written FBGs were written in Corning SMF-28 and Sumitomo Z-fiber both with and without hydrogen loading. Defect FL was used to determine the kinds of defects and their spatial distribution within the fiber. FBGs written in Z-fiber showed strong E_{δ}' and weak Si-based NBOHC defects. For hydrogen-loaded Z-fiber neither of these defects were present after the writing process. The similar spectra from the core and cladding also indicate that fluorine doping in the cladding does not play a large role, if any, in the creation and or passivation of these defects both with and without hydrogen loading.

The case of FBGs written in SMF-28 fibers is more complicated. The core region of SMF-28 contains Ge and because of this, there was a distinct change in the NBOHC FL represented by an overlapping Si-based and Ge-based NBOHC FL. In FBGs without hydrogen-loading the core still contains E_{δ}' defects but an equivalent fiber with hydrogen loading does not show this defect FL but rather an increase in the NBOHC FL. In the cladding, which contains no Ge, the results are consistent with those of Z-fiber, as expected since they are both all-silica glass.

Acknowledgment

The authors acknowledge support of this work by the National Science Foundation under Grant No. DMR 0801786.

#173851 - $15.00 USD Received 7 Aug 2012; revised 16 Oct 2012; accepted 17 Oct 2012; published 25 Oct 2012